Energy Loss and Effective Charge of He, C, and Ar Ions below 10 MeV/amu in Gases*

F. W. MARTIN AND L. C. NORTHCLIFFE
Department of Physics, Yale University, New Haven, Connecticut
(Received June 6, 1962)

The energy loss associated with the passage of typical heavy ions through various gases has been measured as a function of gas thickness. The ions enter an absorber cell with initial energies of about 10 MeV/amu, held fixed by a magnetic analyzer; the final energy of the ions is determined by analyzing the emergent beam with a magnetic spectrograph. Range-energy curves are obtained for He, C, and Ar ions in H_2, N_2, and Ar and for C ions in CH_4 and He. Over-all accuracy is about 1%. The mean ionization potentials of H_2, N_2, and Ar are determined to be 18.3±2.6, 79±7, and 190±17 eV, respectively. From the stopping power for C and Ar ions relative to that for He ions, their fractional effective charge is computed. Plots of the square of the fractional effective charge as a function of the ratio of the velocity of an ion to that of its own first K electron are in agreement with similar plots for heavy ions in aluminum and oxygen, with one exception, the case of Ar ions in H_2.

I. INTRODUCTION

THE stopping of charged particles more massive than protons in the region of ion energy between 1 and 10 MeV/amu has been the subject of active investigation in recent years, primarily because of the need for energy loss corrections in the interpretation of experiments involving heavy ions. The published measurements include results for ions as heavy as argon in a variety of solid materials: photographic emulsion,[1,2] plastics,[3] aluminum,[4–6] and other metals.[5,7,8] But the only gaseous material for which such data are available has been oxygen.[8] While the energy loss of an ion in a given material can be predicted crudely from data for the energy loss of protons in the same material,[9] an accurate prediction must include allowance for the partial neutralization of the charge of the ion and this cannot be calculated accurately at present. The need for experimental measurements in a wider variety of gases is apparent.

The work reported here provides measurements of the energy loss of He^4, C^{12}, and Ar^{40} ions in the gases H_2, N_2, and Ar, and of C^{12} ions in He and CH_4. The mean ionization potentials of the gases are determined from the data for the He ions, and the effective charge of the C and Ar ions in the gases is inferred by comparison of the stopping power for He ions with that for C or Ar ions. In all cases but one, Ar ions in H_2, the fractional effective charge (i.e., the effective charge divided by the nuclear charge) is found to be the same as that in aluminum and oxygen at the same value of the velocity ratio v/v_k, where v_k is the velocity of the first K electron of the ion.

II. APPARATUS AND METHOD OF MEASUREMENT

A schematic plan view of the apparatus is shown in Fig. 1. The energy of the ions before they entered the range cell was held constant by the magnetic deflection system of the accelerator. In the range cell they passed through a measured thickness of gas, and in the magnetic spectrograph their energy after leaving the cell was determined. Through repeated measurements with various gas thicknesses the relationship between the exit energy of the ions and the gas thickness (essentially the range-energy relation) was determined. It should be noted that this measurement differed from the usual range-energy measurement in which the exit energy is fixed (at zero) and the input energy is varied. Measurement of the total range was not attempted because multiple scattering in the range cell reduced the current

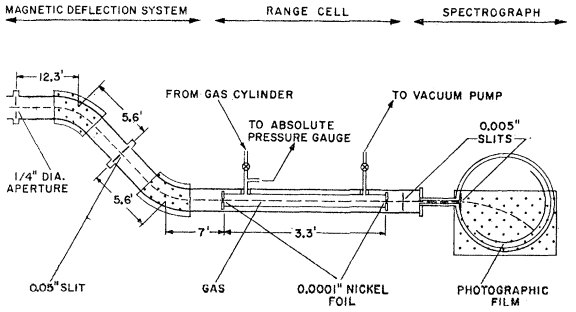

FIG. 1. Schematic plan view of the apparatus (not to scale). The path of the ions is shown by the dashed line, and the dotted areas represent regions of uniform magnetic field perpendicular to the plane of the sketch. Not shown are a pair of quadrupole focusing magnets between the aperture and the first magnet and a second pair between the second magnet and the range cell.

* This work was supported by the U. S. Atomic Energy Commission. A preliminary report was given in Bull. Am. Phys. Soc. 6, 470 (1961).

[1] H. H. Heckman, B. L. Perkins, W. G. Simon, F. M. Smith, and W. H. Barkas, Phys. Rev. **117**, 544 (1960).
[2] P. G. Roll and F. E. Steigert, Nuclear Phys. **16**, 534 (1960).
[3] P. E. Schambra, A. M. Rauth, and L. C. Northcliffe, Phys. Rev. **120**, 1758 (1960).
[4] W. E. Burcham, Proc. Phys. Soc. (London), **A70**, 309 (1957).
[5] Yu. Ts. Oganesyan, J. Exptl. Theoret. Phys. (U.S.S.R.) **36**, 936 (1958) [translation: Soviet Phys.—JETP **8**, 661 (1959)].
[6] L. C. Northcliffe, Phys. Rev. **120**, 1744 (1960).
[7] E. L. Hubbard, University of California Radiation Laboratory Report UCRL-9053, 1960 (unpublished). This reference contains unpublished data obtained by J. R. Walton and E. L. Hubbard, T. Sikkeland, and J. Gilmore.
[8] P. G. Roll and F. E. Steigert, Nuclear Phys. **17**, 54 (1960).
[9] W. Whaling, in *Handbuch der Physik*, edited by S. Flügge (Springer-Verlag, Berlin, 1958), Vol. 34, p. 193.

of ions entering the spectrograph at low exit energies to impractically small levels.

In the magnetic deflection system, ions emerged from a circular aperture (typically $\frac{1}{4}$ in. in diam), traveled about 12 ft through a pair of quadrupole magnets to the first deflecting magnet, and then approximately 6 ft further to an energy selection slit (typically 0.05 in. in width). The system was designed to focus ions of a given energy, emerging from the aperture at small angles, onto a vertical line at the energy slit. The second deflecting magnet steered the ions into the apparatus. In practice, the slit and the aperture were set to minimum sizes consistent with the required ion current and the field of the first magnet adjusted for maximum ion current. The current in the magnet was then held constant throughout a run by electronic regulation of the magnet voltage and by occasional manual adjustment (to compensate for temperature-induced changes in resistance). The current was monitored at all times and maintained constant within 0.1%.

The range cell consisted of a copper tube 2 in. in diam and 40 in. in length rigidly supported inside a copper vacuum pipe 4 in. in diam. So as to maintain thermal contact with the outer pipe, the range cell was soldered to two brass supports each approximately $\frac{3}{4}$ by $1\frac{1}{2}$ in. in cross section. At each end of the cell there was a nickel window, 0.0001 in. in thickness, curved into a cylindrical form (of $\frac{1}{4}$ in. radius) in order to withstand up to 2.5 atm of gas pressure. The largest energy loss in the foils was about 10% of the input energy and occurred for the case of argon ions nearly stopping in the second foil.

The gases were grades whose purity was specified to be 99.9% or better by their manufacturers, except for methane (99%). During each measurement the inlet and exhaust gas valves were closed, so that a constant amount of gas remained within the cell. The pressure of the gas was measured with a Wallace and Tiernan absolute pressure gauge and the room temperature with a mercury thermometer. During some runs the temperature of the range cell itself was determined to within 0.5°C by measuring the current through a reverse-biased germanium junction diode clamped to the exterior of the cell halfway between the brass supports. Although abrupt changes in temperature of up to 0.3°C magnitude and 30-sec duration were observed when the gas pressure was changed, the temperature measured in this way never differed from room temperature by more than 0.7°C.

The magnetic spectrograph has been described in detail elsewhere.[6] After sharp collimation the ions are deflected by a uniform magnetic field (monitored and measured with a proton resonance probe) and detected on a strip of 16-mm motion picture film, all in a rigidly determined and accurately known geometric arrangement. The relationship between deflection and orbit radius is accurately known.

III. REDUCTION OF DATA AND RESULTS

The computation of particle energies from the deflections in the spectrometer, facilitated by use of an IBM-610 computing machine, followed the procedure described elsewhere[6]; the basic formula and the corrections for film shrinkage, edge effects of the magnetic field, and relativistic mass increase were the same.

A special correction was necessary when the distribution of ion energies entering the spectrometer was appreciably broadened by straggling. Because of the nonlinear dispersion of the spectrometer the distribution of ion deflections did not have the same shape as the distribution of ion energies, and the energy corresponding to the most probable deflection differed from the most probable energy of the ions by an amount ΔE. On the assumptions that the energy distribution is Gaussian and that the observed optical density at a point on the film is proportional to the number of ions striking the film per unit area,[10] a formula was derived expressing ΔE in terms of the maximum of the distribution in optical density and of either the upper or lower half maximum. The average of the values of ΔE computed using the two half maxima for a line was taken for a correction. The correction increased with decreasing ion energy. Although it reached 3.3% of the measured energy in the worst case it was always less than 0.05 MeV/amu in magnitude.

The energy measured in the spectrometer was that of ions leaving the rear nickel foil. To determine the energy of the ions as they emerged from the gas it was necessary to correct for the loss in the foil. Such corrections were computed for helium and carbon ions using experimental range data.[8] For argon ions no data were available and an estimate was made.[11]

[10] The first assumption is nearly true according to theory. See, for example, R. D. Evans, *The Atomic Nucleus* (McGraw-Hill Book Company, Inc., New York, 1955), Chap. 22, Sec. 5. To test the second assumption, it was employed to calculate the number of ions per unit energy using the photographic densities measured on typical films and the spectrometer dispersion formula [derived from Eq. (1) of reference 6]; the energy distributions were found to be Gaussian. Since the peak densities of most of the lines were much less than the saturation density of the film the second assumption is in agreement with the exponential approach to saturation density found for alpha particles by S. Kinoshita, Proc. Roy. Soc. (London), **A33**, 44, (1909) and G. H. Briggs, *ibid.* **A114**, 316 (1927).

[11] The estimate was based on the assumption that the range difference (defined in footnote 14) for any ion in nickel is proportional to the range difference for that ion in aluminum. The approximate truth of the assumption in the case of helium ions, as well as the constant of proportionality, was found from the data of references 6 and 8. The range differences for argon ions in aluminum could be computed using Eq. (9) of reference 6. (The value of Δ used in this equation was extrapolated from a table of values of Δ for ions up to neon, computed using Table II of the reference.) The range difference curve for argon ions in nickel was then obtained using the constant of proportionality. The curve was fitted with a polynomial which was differentiated to give, for the loss in the rear nickel foil, the formula

$$\Delta\mathcal{E}=\Delta D/(-3.137+0.0126\mathcal{E}-0.0289\mathcal{E}^2),\quad 2<\mathcal{E}<10,$$

in which ΔD was the measured thickness of the foil (2.14 mg/cm^2) and $\mathcal{E}$ the energy per unit mass of the argon ion (in MeV/amu). This result agrees (within about 6%) with the estimate made from emulsion data in reference 7.

In the case of He ions in H_2 the pressure of the gas within the range cell could not be increased enough to stop the ions completely. Therefore an appropriate thickness of aluminum foil was sometimes placed in front of the first nickel foil. It was then necessary to compute the equivalent thickness L of helium which would reduce the entrance energy to the gas by the same amount as it actually decreased upon introduction of the aluminum. The equivalent thickness L_a of the aluminum and first nickel foil was determined from the energy loss of the ions in aluminum[6] and nickel[8] and from the range data obtained in the gas without the aluminum degrader. The equivalent thickness L_b of the nickle foil, when the energy of the ions traversing it was increased by removing the aluminum, was similarly determined and subtracted from L_a. The difference, L_a-L_b, was added to the gas thickness. As a consistency check, data for He ions in N_2 and C ions in H_2 were also taken with aluminum degraders and analyzed in the same manner even though the ions could be completely stopped in the cell. In the region of overlap at the lower energies where data were obtained both with and without the degrader the agreement was found to be satisfactory.

In four runs, a small shift of all range values taken after some point of time, relative to those taken before, was observed. Since the gas thickness for successive points deliberately was varied so as to provide more or less uniform and simultaneous accumulation of data throughout the entire range, the shift appeared as a sudden displacement of the whole experimental curve, without change in its shape. Such shifts can be attributed to changes in the average energy of the ions entering the range cell, by amounts consistent with the energy resolution of the magnetic analysis system. (Typical energy changes were 0.03 MeV/amu and the largest was 0.04 MeV/amu.) For the case of He ions in N_2, the shift occurred between data taken before and after a 15-h shutdown. For Ar ions in H_2, it occurred when the accelerator exit aperture was enlarged. Critical adjustments of the accelerator by its operators probably caused the other two shifts observed (with C ions in N_2 and Ar). The amount of the range shift was added to data taken after the time when the shift occurred.

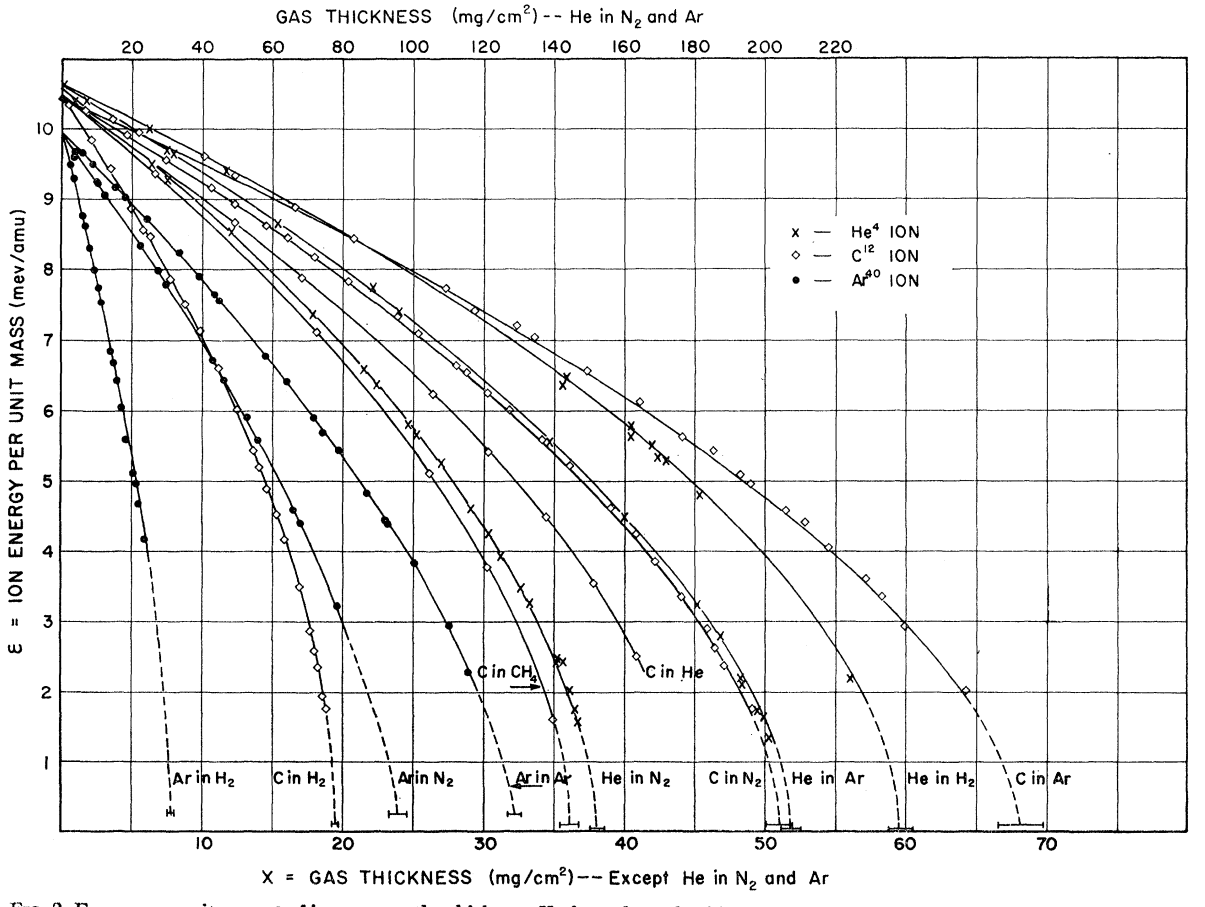

FIG. 2. Energy per unit mass ε of ions versus the thickness X of gas through which they have passed. For each curve the energy of the ions as they enter the gas is constant. The error bars near $\varepsilon=0$ represent gas thicknesses over which the ion current decreased rapidly to zero, and the dashed curves are plausible interpolations. For clarity, only typical points are shown. Note the smaller scale for the case of He ions in N_2 and Ar.

TABLE I. Experimental uncertainties. The estimates include allowances for possible systematic errors.

Origin of uncertainty	Estimate of magnitude	Equivalent error in $\mathcal{E}$ or X
Accuracy of magnetic field	±0.1%	
Magnetic field error		±0.02 to ±0.003 MeV/amu
Choice of line center—		
for undeflected beam	±0.015 mm	
lines less than 1 mm wide	±0.015 mm	
lines more than 1 mm wide	±0.02 to ±0.1 mm	
Line position errors		±0.06 to ±0.002 MeV/amu
Thickness of rear nickel foil—		
error in average	±0.4%	
fluctuations from average	±0.8%	
effects of curvature of foil	±3%	
Accuracy of slope of range-energy data for ions in nickel	±6%	
Rear nickel foil errors		±0.06 to ±0.003 MeV/amu
Constancy of input energy	±0.02 to ±0.04 MeV/amu	
Error caused by input energy error		±0.05 to ±0.6 mg/cm²
Nonlinearity of absolute pressure gauge	±0.05 in. Hg	
Accuracy of temperature of range cell	±0.5°C	
Length of range cell	±0.05 cm	
Pressure, temperature, and length errors		±0.01 to ±0.4 mg/cm²
Local heating error		0 to −0.82 mg/cm²
Error in effective thickness L of aluminum and front nickel foil		±0.18 to ±1.2 mg/cm²

The results are presented in Fig. 2. Horizontally is shown the thickness X of the gas in mg/cm² and vertically the energy of the ion divided by the rest mass of its nucleus in amu, giving the quantity $\mathcal{E}$ in MeV/amu. The error bars near $\mathcal{E}=0$ represent gas thicknesses over which ion current through the range cell, measured on a pair of slit jaws beyond the cell, decreased rapidly to zero. The dashed lines are a plausible interpolation.

IV. ACCURACY

The known experimental uncertainties are listed in Table I along with estimates of their magnitude which allow for both random fluctuations and possible systematic errors. Although the individual estimates include systematic errors of definite amounts, the amounts are not known and it is unlikely that they would all cause final errors of the same sign. Therefore, the individual uncertainties were treated as probable errors, and the equivalent uncertainties in $\mathcal{E}$ or X were combined quadratically. The resultant uncertainties for related groups of errors are also listed in Table I. The inclusion of estimates of systematic error causes the over-all uncertainties to be larger than the fluctuations in the data.

Many of the sources of error could be represented, for a given ion-gas combination, by a constant uncertainty in X over the energy range of the experiment. The line position errors were most serious at high energies because the deflections in the spectrometer then were smallest. The magnetic field error, a constant percentage of the energy, was also largest at high energies. The temperature and length errors increased in proportion to the gas thickness and at times became larger than the pressure error (which was constant). The largest error was in the effective thickness L of the energy degrading arrangement when it was used.

In the case of C ions in N_2 and Ar and of He ions in N_2 the current of ions was probably large enough to raise the temperature at the center of the cell significantly above that measured at its walls. In an attempt to estimate the magnitude of the rise, the effect of a hot wire placed on the axis of the range cell was investigated. The temperature rise above the wire was measured with a disc thermistor of 0.1-in. diam as a function of gas pressure and power dissipated in the wire. These data indicate a maximum temperature increase of 3.8°C at the estimated levels of power dissipated by the ions.

Because it is not known what fraction of the measured ion current passed through the first nickel foil, the estimates of power dissipation and temperature increase may be too large by as much as a factor of 10. The spuriously high energies associated with the temperature rise cause a systematic error of known direction. The error bars in Fig. 4 include the above-described upper limit added directly at only one end.

In the case of He ions in Ar it was determined that an increase by a factor of 7 over the normal current of ions decreased the gas thickness by only 0.6%. The

TABLE II. Values of β and δ. The slope of a straight line in Fig. 3 is equal to β. The quantity δ, defined by Eq. (2), is $1/\beta$ times the deviation of the points of Fig. 3 from a straight line. Range differences may be computed using the formula $X(\mathcal{E})-X(10)=\beta[X_p^{Al}(\mathcal{E})+\delta]$. The values of δ listed here correspond to the smooth curves of Fig. 4.

	$\mathcal{E}$ (MeV/amu)		10	9	8	7	6	5	4	3	2
	X_p^{Al}(mg/cm²)		0	28.6	54.9	78.8	100.2	119.0	135.3	148.8	159.4
Ion	Gas	β	Values of δ (mg/cm²) for the above values of $\mathcal{E}$ or X								
He^4	H_2	0.3293	0	0.1	−0.2	−0.8	−1.7	−2.8	−4.0	−5.4	
He^4	N_2	0.8177	0	0.2	0.4	0.5	0.6	0.5	0.4	0.1	−0.3
He^4	Ar	1.099	0	−0.2	−0.3	−0.4	−0.6	−0.6	−0.2	0.4	1.0
C^{12}	H_2	0.1105	0	0.1	0.0	−0.1	−0.3	−0.7	−1.4	−2.3	−3.2
C^{12}	CH_4	0.1992	0	0.2	0.3	0.2	0.0	−0.3	−0.6	−0.9	−1.3
C^{12}	He	0.2451	0	0.5	0.8	1.0	1.0	0.9	0.7	0.4	
C^{12}	N_2	0.2811	0	−0.1	−0.2	−0.3	−0.3	−0.5	−0.6	−0.8	−0.9
C^{12}	Ar	0.3661	0	−0.1	0.0	0.2	0.6	1.1	1.6	2.1	2.7
Ar^{40}	H_2	0.04595	0	−0.7	−1.4	−1.9	−1.7	−1.1	−0.5		
Ar^{40}	N_2	0.1339	0	−1.1	−1.7	−1.7	−1.1	0.0	1.5	4.3	
Ar^{40}	Ar	0.1863	0	−1.3	−2.4	−3.1	−3.2	−2.6	−1.1	0.9	

decrease in thickness at the normal current was assumed to be negligible.

V. ANALYSIS AND DISCUSSION

A. Systematic Tendencies

The most noticeable characteristic of the curves of Fig. 2 is their similarity in shape. To test the extent of this similarity all the curves were compared to a standard, based on the range-energy curve for protons in aluminum, which has been fitted by an accurate empirical formula[12,13]:

$$X_p^{Al}(\mathcal{E})=171.11-\frac{2.880\mathcal{E}^2}{0.6833+\log_{10}\mathcal{E}}, \qquad 17.86>\mathcal{E}>2.657, \quad (1)$$

$$=171.11-3.883\mathcal{E}^{1.5874}, \quad 2.657>\mathcal{E}>1.12.$$

Here $X_p^{Al}(\mathcal{E})$ is the thickness of aluminum in mg/cm² traversed by a proton while slowing from 10 MeV per amu to $\mathcal{E}$ MeV/amu, a quantity which can be interpreted as a range difference.[14] In Fig. 3 the thickness $X(\mathcal{E})$ traversed in the range cell by an ion slowed to energy $\mathcal{E}$ per unit mass is plotted against $X_p^{Al}(\mathcal{E})$. The close fit to the straight lines indicates that all the range curves have nearly the same shape as the curve for protons in aluminum. In fact, range differences estimated simply by multiplying Eq. (1) by the slopes of these lines deviate from the measured range differences by less than 4% of the full range of the ion. The values β of these slopes are given in Table II.

The similarity in shape of the curve for He ions and those for the heavier ions in a given gas may be interpreted by recalling that for a given initial velocity in a given material the range of an ion of fixed charge is proportional to the square of its charge and inversely proportional to its mass. Therefore, if both ions have a constant charge, their curves will have exactly the same shape. Since the He ion is stripped of both its electrons above $\mathcal{E}=2$ MeV/amu,[15] the close similarity of shape

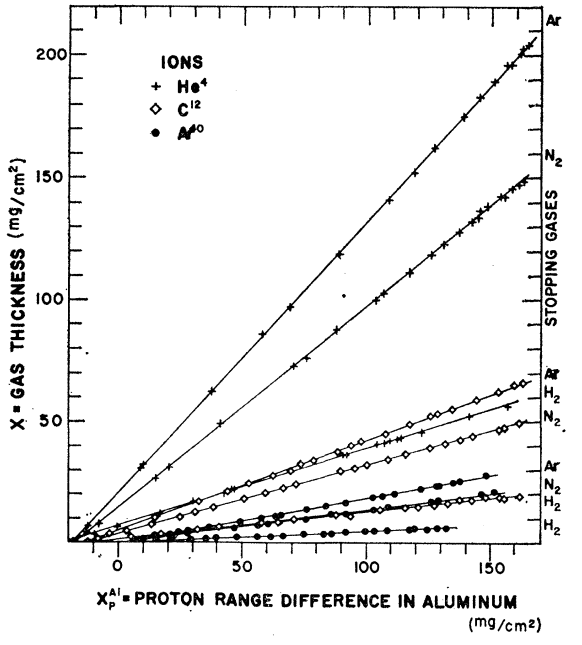

FIG. 3. Demonstration of the similarity in shape of the heavy ion and proton range-energy curves. The quantity X is the thickness of gas traversed by an ion while slowing from its fixed initial energy to an energy (per unit mass) of $\mathcal{E}$ MeV/amu, and X_p^{Al} is the thickness of aluminum traversed by a proton while slowing from 10 MeV/amu to $\mathcal{E}$ MeV/amu.

[12] H. Bichsel, Phys. Rev. **112**, 1089 (1958).

[13] H. Bichsel, R. F. Mozley, and W. A. Aron, Phys. Rev. **105**, 1788 (1957).

[14] By the range difference $X(\mathcal{E})$ is meant the quantity $R(\mathcal{E}_0)-R(\mathcal{E})$, where $R(\mathcal{E})$ is the range of ions with energy $\mathcal{E}$ per unit mass (in MeV/amu) and $\mathcal{E}_0$ is a fixed reference value of $\mathcal{E}$. The value taken for $\mathcal{E}_0$ for heavy ions is their energy per unit mass as they enter the gas; for protons in aluminum $\mathcal{E}_0=10$ MeV/amu.

[15] Measurements of the charge of He ions are summarized in Evans, reference 10, p. 636. Although the rms charge of a group of He ions is not exactly $2e$ at any energy in the range of this experiment, the difference from $2e$ is too small to be significant.

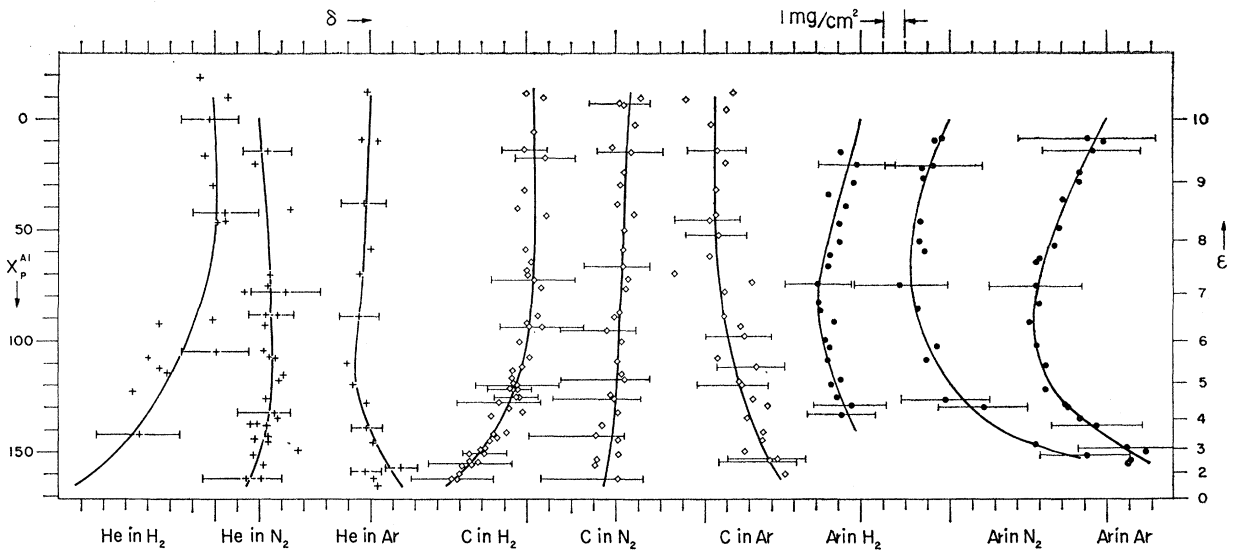

FIG. 4. Differences between the expanded curves X/β for ions in gases and the curve X_p^{Al} for protons in aluminum. The deviations from vertical are interpreted in the text in terms of the ionization potentials of the gases and the effective charges of the ions. Except for 12 points in the data for He ions in N_2 excluded because of local heating effects, all of the data for each curve are shown.

here implies that the charge of the C or Ar ions does not vary greatly in the energy region of the experiment. However, the nearly constant charge is not necessarily the nuclear charge of the ion. In fact, if the nuclear charge is used to compute the value of β for argon ions from its value for helium ions the result is about 30% in error, implying that the argon ion carries several electrons even at the highest energies measured.

To demonstrate that the data of Fig. 3 do not fall exactly on straight lines the difference

$$\delta=(1/\beta)[X(\mathcal{E})-X(10)]-X_p^{Al}(\mathcal{E}) \qquad (2)$$

was computed for each measurement and plotted as a function of X_p^{Al}. The result is shown in Fig. 4. The error bars are of length dX'/β computed from the thickness errors dX and the energy errors $d\mathcal{E}$ using the formula

$$(dX')^2=(dX)^2+[(dX/d\mathcal{E})d\mathcal{E}]^2.$$

Nonlinearities are now apparent and in some cases are greater than the uncertainties. Values of δ for the smooth curves are given for reference in Table II.

The deviation of a particular smooth curve from a straight line can be attributed to the variation of the charge of the ion and to the value of the mean ionization potential I of the gas. Because He ions maintain constant charge, the three curves for He ions can show only ionization potential effects. If the curve for He ions in Al were shown in Fig. 4, it would be a vertical straight line. The fact that the plot for He ions in Ar is curved to the right indicates that $I_{Ar}>I_{Al}$, while the fact that the plots for He ions in H_2 and N_2 are curved to the left indicates that $I_H<I_{Al}$ and $I_N<I_{Al}$. Charge effects can be isolated by comparing the curves for different ions in the same gas. For example, the curves for He and Ar ions in a given gas differ in shape because the Ar ions gradually lose charge as they slow down while the He ions maintain constant charge. (The curves would have the same shape if both ions maintained constant charge.) A more critical and quantitative discussion of these effects is given in the following sections.

B. Mean Ionization Potential

According to the Bethe theory[16,17] the stopping power of a medium with N atoms per cm³ of atomic number Z, for a particle of velocity v cm/sec and charge ze, is given by the expression

$$-(dE/dx)=(4\pi e^4/m_0)NZ(z^2/v^2)\ln(2m_0v^2/I). \qquad (3)$$

Evaluated numerically in the units used here this becomes

$$\frac{d\mathcal{E}}{dX}=-2.762\times10^{17}\frac{z^2}{m}\frac{Z}{A}\frac{1}{v^2}\ln\left(1.137\times10^{-15}\frac{v^2}{I}\right), \qquad (4)$$

in which m is the mass of the ion in amu, A is the atomic weight of the material, and I the mean ionization potential of Bethe's theory in electron volts. The assumptions of the theory are met only when the ion moves more swiftly than the K electrons of the material, i.e., when

$$v>Zv_0=Zc/137, \quad \mathcal{E}>0.025Z^2, \qquad (5a)$$

Thus G. H. Henderson [Proc. Roy. Soc. (London) **A109**, 157 (1925)] found that one ion in 161 retained an electron at a velocity corresponding to $\mathcal{E}=1.9$ MeV/amu.

[16] H. A. Bethe and J. Ashkin, in *Experimental Nuclear Physics*, edited by E. Segrè (John Wiley & Sons, Inc., New York, 1953), Vol. I.

[17] H. A. Bethe, Ann. Physik **5**, 325 (1930).

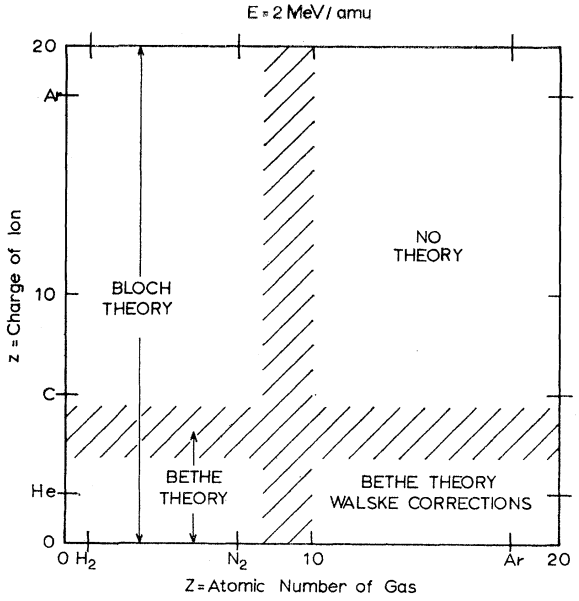

FIG. 5. Diagram showing the regions of applicability of various theories for ions with $\mathcal{E}=2$ MeV/amu. In the region to the right of $Z=9$ inequality (5a) is not satisfied, and in the region above $z=4.5$ inequality (5b) is not satisfied. If $\mathcal{E}=10$ MeV/amu, the dividing lines are shifted by about a factor of two towards higher Z and z. *Note added in proof.* For the Bloch theory to give the stopping contribution of the K electrons of the material, inequality (5a) and the further inequality $v>v_0(zZ)^{1/2}$ must be satisfied simultaneously. In this figure the Bloch theory is, therefore, applicable only in a region to the left of both the line $Z=9$ and the hyperbola $zZ=80$.

and when the Born approximation is valid, i.e., when

$$v>2zv_0=2zc/137, \quad \mathcal{E}>0.099z^2. \tag{5b}$$

Figure 5 shows the values of Z and z at which these restrictions become operative when the ion has an energy of 2 MeV per amu of mass. It is seen that the Bethe expression is of doubtful applicability, especially to an argon ion.

A formula has been derived by Bloch for highly charged ions with large velocities.[16,18] Also corrections to Eq. (4) have been computed by Walske for the case of low ionic velocity, provided the charge of the ion is small so that the Born condition is satisfied.[19,20] If Walske's corrections are included Eq. (4) becomes

$$\frac{d\mathcal{E}}{dX}=\frac{-2.762\times10^{17}z^2Z}{mAv^2}\times\left[\ln\left(1.137\times10^{-15}\frac{v^2}{I}\right)-\frac{C_K+C_L}{Z}\right], \tag{6}$$

where C_K and C_L are given in references 19 and 20. (Although the values of C_L are of doubtful accuracy for gases of $Z<30$ they are the only ones available.) Using the abbreviation

$$\mathfrak{L}=-\frac{1}{2.762\times10^{17}}\frac{m}{z^2}\frac{A}{Z}\frac{d\mathcal{E}}{v^2\,dX}, \tag{7}$$

Eq. (6) can be rearranged to read

$$\mathfrak{L}+\frac{C_K+C_L}{Z}=\ln\left(1.137\times10^{-15}\frac{v^2}{I}\right). \tag{8}$$

Since $z=2$ for He ions above $\mathcal{E}=2$ MeV/amu,[15] the left side of Eq. (8) is known and can be plotted as a function of $\ln(v^2/c^2)$ in order to determine I.

Figure 6 shows such plots for He ions in H_2, N_2, and Ar. The values of $\mathfrak{L}$ were obtained by evaluating Eq. (7), using $d\mathcal{E}/dX$ values determined by application of the formula

$$\frac{d\mathcal{E}}{dX}=\frac{1}{\beta}\frac{d\mathcal{E}}{dX_p{}^{\mathrm{Al}}}\left(1+\frac{d\delta}{dX_p{}^{\mathrm{Al}}}\right)^{-1} \tag{9}$$

to the measured slopes of the smooth curves of Fig. 4. The values of $d\mathcal{E}/dX$ obtained are plotted for reference in Fig. 7. The uncertainties in $\mathfrak{L}$ were obtained by estimating the maximum and minimum slopes consistent with the errors displayed in Fig. 4.

The uncorrected values of $\mathfrak{L}$ in Fig. 6 are seen to be systematically lower than the corrected points. The values of I derived from the uncorrected $\mathfrak{L}$ values would be erroneously high and become higher as the energy of the ion decreased.

The corrections were computed using the parameters listed in Table III. No corrections were needed for H_2 and those for the L shell of N_2 were estimated to be small. In the case of Ar the deviation of the corrected points from a straight line below $\mathcal{E}=5$ MeV/amu may

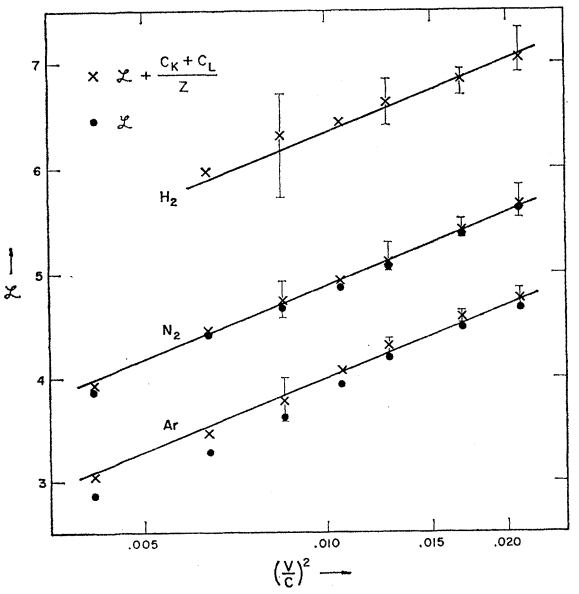

FIG. 6. Corrected and uncorrected values of the logarithm in the Bethe formula. Ionization potentials determined from the positions of the straight lines are given in Table III.

[18] F. Bloch, Ann. Physik **16**, 285 (1933).
[19] M. C. Walske, Phys. Rev. **88**, 1283 (1952).
[20] M. C. Walske, Phys. Rev. **101**, 940 (1956).

be due to the inaccuracy of the appreciable L shell corrections applied. Straight lines of slope given by Eq. (8) are fitted to the corrected values of $\mathcal{L}$. The mean ionization potentials determined from these lines are given in Table III with errors estimated by means of parallel straight lines through the ends of the smaller error bars. For comparison the conclusions of a review of early data for natural alphas[21] ($\mathcal{E}<2.5$ MeV/amu) are shown.[21a]

C. Effective Charge

It is convenient to discuss small differences in the shape of curves for different ions in the same material in terms of an empirical parameter called the effective charge of the ion. This quantity is calculated from the ratio of the experimental stopping powers for the ion and for a reference ion of known charge (at the same velocity in the same substance) through use of the defining formula

$$[(z_{\text{eff}})^2]_{\text{ion}}^{\text{gas}}=\left[m\frac{d\mathcal{E}}{dX}\right]_{\text{ion}}^{\text{gas}}\Big/\left[\frac{m}{z^2}\frac{d\mathcal{E}}{dX}\right]_{\text{ref. ion}}^{\text{gas}}. \qquad (10)$$

TABLE III. Values of the mean ionization potential. For comparison, the values of Bogaardt and Koudijs are also shown. The shell correction parameters used in deriving the ionization potentials from the present data are included.

Gas	Shell correction parameters $\mathcal{E}/\eta_K$	θ_K	$\eta_L/\mathcal{E}$	θ_L	Values of I in eV: Present experiment	Bogaardt and Koudijs
H_2					18.3±2.6	17.1±0.3
N_2	1.11	0.66			79±7	76.2±3.8
Ar	7.76	0.75	0.211	0.35	190±17[a]	226.8±2.3[a]

[a] Since L-shell corrections were not available to Bogaardt and Koudijs, agreement of these values is not to be expected.

He ions may be taken as reference ions in the evaluation of Eq. (10) since their charge is known to be $z=2$ at the ion velocities encountered in this experiment.[15]

By substitution of Eq. (6) into Eq. (10) it can be seen that $(z_{\text{eff}})^2$ is the value of z^2 required in Eq. (6) to give agreement with the observed stopping powers. Beyond this the physical interpretation of z_{eff} is less certain. The quantity z_{eff} is the rms charge of the ion if Eq. (6) (or any other equation having the same dependence on z and m) gives a true description of the energy loss of an ion of charge z. However, this interpretation may not be valid if the use of Eq. (6) is not justified, as would be the case if inequality (5b) is not satisfied or if the electrons of the stopping material penetrate the charge cloud of the ion. On the assumption that the result of an exact calculation would not differ much from Eq. (6), the effective charge may be taken as a good approximation to the actual charge.[22]

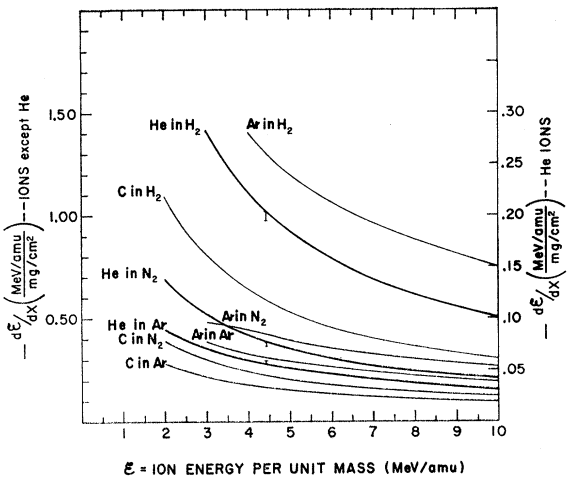

FIG. 7. Values of $d\mathcal{E}/dX$ computed from the data using the graphically determined slopes of the smooth curves of Fig. 4 in Eq. (9). Estimated accuracy is plus or minus 1–3% at 6 MeV/amu and 5–10% at the low-energy end of a curve. The three points at 4.4 MeV/amu are the data of J. E. Brolley and F. L. Ribe, Phys. Rev. 98, 1112 (1955). Note the larger scale for He ions.

Figure 8 shows the values of $\gamma^2=(z_{\text{eff}}/z_0)^2$ (where z_0 is the atomic number of the ion), given by Eq. (10) for the $d\mathcal{E}/dX$ values of Fig. 7, plotted as a function of v/v_k (where v_k is the velocity of the first K electron of the ion). The indicated uncertainties are based on

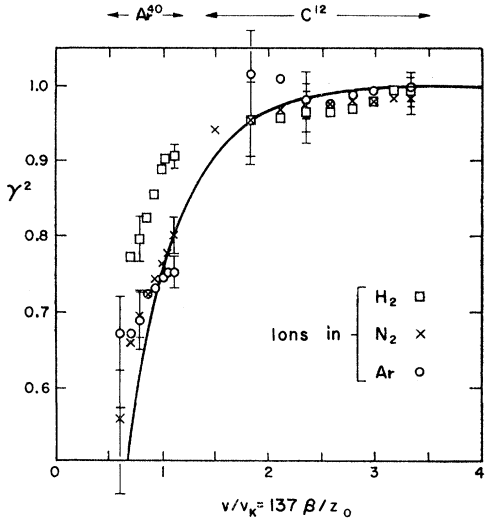

FIG. 8. Effective charge of carbon and argon ions in three gases. The quantity γ^2 is the square of the ratio of the effective charge of the ion to its atomic number. The horizontal coordinate is the velocity of the ion divided by the velocity of its first K electron. The smooth curve is a best fit to comparable data for heavy ions in aluminum.

[21] M. Bogaardt and B. Koudijs, Physica 18, 249 (1952).

[21a] *Note added in proof.* H. Bichsel independently analyzed the data of this experiment and sent us the I values he obtained for H_2 and N_2. The inadequacy of a nonrelativistic conversion from $\mathcal{E}$ to v was revealed in the attempt to reconcile one of our initial I values with his. The I values quoted in Table III are in agreement with those obtained by Bichsel.

[22] The validity of this interpretation for oxygen ions in the region $1<\mathcal{E}<8$ MeV/amu is shown by the results discussed in the subsection on "Effective Charge" in reference 6.

subjective estimates of the limiting slopes that could fit the scatter of points in Fig. 4. The uncertainty caused by systematic errors generally is smaller than these estimates. The solid line shown is a best fit to the values of γ^2 for heavy ions in aluminum [given by Eq. (10) of reference 6]. The data of this experiment are in substantial agreement with the solid line in all cases except that of Ar ions in H_2. Similar agreement exists with data for heavy ions in oxygen.[8] The value of γ^2 thus appears to be independent of the atomic number and physical state of the stopping substance, the only exception occurring in the case of a gas at low Z.

The unusually high charge of Ar ions in H_2 can be understood qualitatively in terms of the theory of Bohr and Lindhard,[23] which was constructed to describe the charge of fission fragments at somewhat lower velocities. If the loss and capture cross sections σ_l and σ_c are calculated at $v/v_k=1$ using Eqs. (4.5) or (4.6) and (4.2)[24] of their paper it is found that σ_l is much larger than σ_c for carbon or argon ions in hydrogen, while the cross sections are more nearly equal for these ions in nitrogen or argon gas. In terms of this theory, the reason for the anomalous behavior in hydrogen is that the loosely bound electron of hydrogen is liberated at a large ion-to-atom distance and is seldom available for capture, while in the higher Z gases some of the electrons of the atom are released at ion-to-atom distances at which escape from the ion is impossible.

VI. SUMMARY

Using a magnetically analyzed input beam with energy of about 10 MeV/amu, the exit energy of various heavy ions from measured thicknesses of certain gases was determined by a magnetic spectrograph. Range differences were measured with an accuracy of about 1% for He, C, and Ar ions passing through H_2, N_2, and A gas and for C ions in He and CH_4. The range-energy curves are varied in scale but very nearly the same in shape. The variations in scale reflect the differences in the charge of the various ions and in the mean ionization potential of the gases. The small deviations in shape are caused partly by the differences in ionization potential and partly by differences in the velocity dependence of the charge of the ion.

The Bethe theory as corrected by Walske for low ionic velocities was used to determine mean ionization potentials for H_2, N_2, and Ar from the He ion data, although the applicability of the correction is questionable in the case of Ar. The corrected Bethe formula also served as the basis for computation of the effective charge of carbon and argon ions in H_2, N_2, and Ar. At the same values of v/v_k the values found for the fractional effective charge were substantially the same as those previously found for heavy ions in aluminum and oxygen, except in H_2 gas where Ar ions had higher effective charge. From the viewpoint of the theory of Bohr and Lindhard, the anomaly in H_2 is expected because of the scarcity of capturable electrons.

ACKNOWLEDGMENTS

The efforts and cooperation of the operating staff of the Heavy Ion Accelerator, under the direction of Professor R. Beringer, are gratefully acknowledged. We also wish to thank Dr. H. Bichsel for his stimulating correspondence and in particular for sending the results of his independent determination of the ionization potentials from these data.

[23] N. Bohr and J. Lindhard, Kgl. Danske Videnskab. Selskab, Mat.-fys. Medd. 28, No. 7 (1954).

[24] In this equation, the effective quantum number ν is substituted for $Z^{1/3}$.